Electrospun Tropoelastin for Delivery of Therapeutic Adipose-Derived Stem Cells to Full-Thickness Dermal Wounds

Hans Machula,[1] Burt Ensley,[2] and Robert Kellar[1–3,*]

[1]Biological Sciences, Northern Arizona University, Flagstaff, Arizona.
[2]Protein Genomics, Sedona, Arizona.
[3]Development Engineering Sciences, Flagstaff, Arizona.

Robert S. Kellar, PhD

Submitted for publication October 11, 2013. Accepted in revised form January 20, 2014.

*Correspondence: 708 North Fox Hill Road, Flagstaff, AZ 86004 (e-mail: rskellar@des-company.com).

Objective: To evaluate the physiological effects of electrospun tropoelastin scaffolds as therapeutic adipose-derived stem cell (ADSC) delivery vehicles for the treatment of full-thickness dermal wounds.
Approach: Using the process of electrospinning, several prototype microfiber scaffolds were created with tropoelastin. Initial testing of scaffold biocompatibility was performed *in vitro* through ADSC culture, followed by scanning electron microscopy (SEM) for assessment of ADSC attachment, morphology, and new extracellular matrix (ECM) deposition. The wound healing effects of ADSC-seeded scaffolds were then evaluated in a murine dermal excisional wound model.
Results: For the *in vitro* study, SEM revealed exceptional biocompatibility of electrospun tropoelastin for ADSCs. In the wound-healing study, ADSC-treated groups demonstrated significantly enhanced wound closure and epithelial thickness compared to controls.
Innovation: This is the first report on the use of tropoelastin-based biomaterials as delivery vehicles for therapeutic ADSCs.
Conclusion: We have demonstrated that tropoelastin-based ADSC delivery vehicles significantly accelerate wound healing compared to controls that represent the current clinical standard of care. Furthermore, the unique mechanical and biochemical characteristics of tropoelastin may favor its use over other biological or synthetic scaffolds for the treatment of certain pathologies due to its unique intrinsic mechanical properties.

INTRODUCTION

The optimal treatment for full-thickness wounds is to approximate the wound edges as soon as possible, allowing for healing via first intention.[1] In some cases, however, approximation of the wound borders is not feasible. Autologous skin grafting is the gold standard treatment in these scenarios[2] but has its own complications. A new wound must be created in the process of harvesting the autograft, increasing the risk of infection, necrosis, pathological scarring, contraction, and permanent deformity.[1] Furthermore, in patients with severe burns that cover most of the body, autologous skin grafting may not be possible due to an overall scarcity of donor sites.[2]

The few other options include temporary cadaver allografts and xenografts or the application of expensive and sometimes unreliable dermal substitutes, such as Integra (Integra Life Sciences, Plainsboro, NJ) and Dermagraft (Shire, San Diego, CA)[2–3] Simply allowing the wound to heal by second intention may take months or even years[1] and can lead to disfigurement.

DOI: 10.1089/wound.2013.0513

Suboptimal outcomes such as these highlight the need for tissue-engineered skin and/or wound dressings with regenerative properties.

The use of adipose-derived stem cells (ADSCs) has recently shown considerable potential for accelerating wound closure. Adipose tissue has been shown to be a significantly more concentrated source of adult stem cells than other tissues, such as bone marrow, circulating blood, or other target organs.[4] The harvesting of ADSCs through lipoaspirate is an easier, less invasive, and a much less painful method than isolation of bone marrow stem cells.[4–5] The relative ease and robustness of ADSC harvest has notable clinical implications, as it may ultimately decrease the *in vitro* culture time required for generation of a therapeutic cell dose.

ADSCs have been shown to accelerate healing through epithelialization, neovascularization, and granulation tissue deposition.[6–7] One established mechanism for this accelerated wound healing is the direct differentiation of ADSCs into endothelial cells,[4] perivascular cells,[6] and fibroblasts.[8] ADSCs also contribute to wound healing via expression of several soluble factors, most notably hepatocyte growth factor,[8] vascular endothelial growth factor,[8] fibroblast growth factor-β,[4,6,7,9] transforming growth factor-β,[9] and keratinocyte growth factor.[8,9] ADSCs also exhibit robust expression of extracellular matrix (ECM) proteins, such as type 1 collagen and fibronectin, thus strengthening the essential acellular components of a wound site.[9]

In order for the regenerative potential of ADSCs to be fully realized, an optimal method for delivering and maintaining these cells in the wound environment is required. ADSC delivery via local injection has indeed produced accelerated wound healing in animal models[6,8] however, the effectiveness of this technique may be diminished by poor retainment of the therapeutic cells in the wound bed.[10] Considering this, a highly promising strategy for ADSC delivery to dermal wounds is the use of a woven membrane or scaffold, upon and within which the cells are cultivated before topical administration. These scaffolds may anchor the therapeutic cell line in the vicinity of the wound, providing maximum therapeutic effect. Such scaffolds can also be tailored to fit within the wound or skin defect,[11] further serving a protective function and providing a large exposure area to the therapeutic cell line. Perhaps most importantly, the use of biomaterial scaffolds far surpasses their mere mechanical use as a support, because cell–scaffold interactions significantly and positively affect the physiology of ADSCs, possibly by mimicking the native ECM.[7]

In the present study, we synthesized native-like scaffolds by electrospinning the human ECM protein tropoelastin. This protein is the soluble precursor to elastin, a major component of healthy skin that is notably absent in scar tissue. Tropoelastin also functions as a matrikine in a wound environment, releasing peptides that are chemotactic for monocytes, macrophages, and neutrophils,[12] as well as endothelial cells,[13] keratinocytes,[14] and fibroblasts.[13] Such elastic peptides have also been shown to induce the proliferation of vascular smooth muscular cells[15] and dermal fibroblasts.[16]

We hypothesized that a scaffold constructed from electrospun human tropoelastin could be populated with ADSCs, and that these cells would proliferate upon and within the scaffold structure and induce a healing response superior to that of control therapy. The growing population of cells would modify and condition the structure by synthesizing and secreting their own ECM molecules onto the matrix, creating a unique "living dressing." This dressing could then be introduced into a wound to protect the site, hold the ADSCs in place, and provide mechanical and biochemical properties that would accelerate closure and healing of a wound. The resulting scar may have mechanical properties far superior to those of a naturally healed scar.

CLINICAL PROBLEM ADDRESSED

The lack of expedient wound closure and poor aesthetic outcomes are significant problems in the clinical setting. A patient with chronic, nonhealing wounds that may persist for months to years, such as nonhealing chronic ulcers, exemplifies these issues. Additionally, if healing does occur, healed tissue can be characterized by extensive scarring and contraction, which inhibits normal movement and renders the healed integument aesthetically unappealing.

MATERIALS AND METHODS

Electrospinning procedure

Recombinant human tropoelastin (rhTE) was a gift from Protein Genomics, Inc. (Sedona, AZ). 1,1,1,3,3,3-Hexafluoro-2-propanol (hexafluoroisopropanol, or HFIP) was obtained from Oakwood Products (West Columbia, SC). For each trial, 100 mg of lyophilized tropoelastin was dissolved into 1 mL of HFIP. The protein solution was loaded into the source solution injector via aspiration with a 1.0 mL syringe, which was then loaded onto the syringe pump set to a 2.5 mL/h ejection rate. Electrospinning was initiated by activation of the

power supply, set to 18–22 kV. The distance from needle to the grounded target was adjusted as needed to facilitate an even spray pattern; typically 8 cm.

Electrospun membranes were crosslinked with vapor-phase glutaraldehyde (GA) for 24 hours (prepared as a 25% glutaraldehyde stock aqueous solution). Membranes were subsequently rinsed with deionized water (Millipore Direct-Q3 purification system, Millipore Corp., Billerica, MA) to remove residual glutaraldehyde.

Sterilization of electrospun membranes

Before *in vitro* biocompatibility experiments were conducted, electrospun scaffolds were disinfected on both sides through irradiation with a 15 W, germicidal ultraviolet (UV) C lamp (Spectroline X-series germicidal lamp, Spectronics Corporation, Westbury, NY).[18] As an added measure of microbial control before the *in vivo* wound-healing experiments, electrospun scaffolds were soaked in 70% ethanol (aqueous) and dried before UVC exposure.[19]

Seeding ADSCs onto electrospun membranes

Cryopreserved ADSCs at passage 1 were provided by American CryoStem Corporation (Eatontown, NJ). Donor cells for the current study were donated from a consenting 36-year-old female patient. Targeting deep subcutaneous deposits, lipoasparate was collected from the left hip. Cells were thawed, transferred to 75 cm^2 tissue culture plates, and incubated (37°C, 5% CO_2, 95% humidity) in 12 mL of MesenCult® mesenchymal stem cell culture media (STEMCELL Technologies, Inc., Vancouver, Canada), supplemented with MesenCult® mesenchymal stem cell stimulatory supplement (10% by volume). Culture used for the murine excisional wound-healing study was supplemented with 50 μg/mL gentamicin, as an extra measure of microbial control. Cell cultures were passaged at 80–90% confluence. Between passage of cells, a half volume of spent medium was exchanged with fresh medium every 2 days.

Biocompatibility studies used both crosslinked and un-crosslinked samples of electrospun rhTE membranes. After disinfection and denucleation, 4-mm membrane samples were placed in separate wells of a sterile, 96-well tissue culture plate. Each well was seeded with 27 μL of 2.26×10^6 cells/mL ADSC suspension (passage 4), providing a final seeding density of 215 cells/mm^2. To each well, 100 μL of media were added, and an additional 100 μL of fresh media was added every 2 days. ADSC-seeded membranes were incubated for a total of 6 days before being transferred to 4% paraformaldehyde for scanning electron microscopy (SEM) preparation. After 24 hours of paraformaldehyde fixation, samples were rinsed and stored in 70% ethanol (aqueous) before SEM processing.

In vivo excisional wound-healing experiments used 8-mm samples of disinfected, denucleated, and crosslinked membranes transferred to a 24-well tissue culture plate and seeded with 175 μL of 7.56×10^5 cell/mL of ADSC suspension (passage 4), providing a final seeding density of 747 cells/mm^2. Samples were incubated for approximately 20 hours (37°C, 5% CO_2, 95% humidity).

Surgical procedure and engraftment of ADSC-seeded scaffolds

Four purpose-bred, female, severe combined immunodeficient (SCID) hairless congenic mice (strain code 488, Charles River Laboratories International, Inc., Wilmington, MA) were used for the *in vivo* studies. All procedures were reviewed and approved by the Institutional Animal Care and Use Committee of Northern Arizona University (protocol number 12-006). Mice were anesthetized via inhalation of isoflurane to effect. For induction, mice were placed in a chamber receiving a 1–2 L/min flow of oxygen with 2–3% isoflurane. Appropriate depth of anesthesia was monitored by absence of response to toe pinch stimuli. Each animal received one intramuscular injection of buprenorphine (3 μg in 0.5 mL sterile saline) for immediate postoperative pain control. Animals were then placed on the sterile surgical field in ventral recumbency atop warming pads and connected to a nose-cone that delivered a 0.5–1 L/min flow of oxygen with 0.5–1.5% isoflurane for maintenance anesthesia.

The mice were randomly assigned into treatment and control groups. One mouse was used for creation of control group wound sites, and three mice were used for treatment group wound sites. Before creation of wound sites, the dorsum was scrubbed with betadine solution and a circular impression was created at each wound site using a sterile, 6-mm biopsy punch with a gentle rotation motion.[19] The center of each impression was grasped and elevated with sterile rat-tooth forceps, and sharp excision of the integument at the circular impression was performed using sterile, curved Castroviejo scissors. Wounds were created in animals $\sim$10 and $\sim$20 mm caudally from the base of the neck and $\sim$7 mm laterally from the spine. Wounds were gently rinsed with sterile saline before application of treatment or control

wound dressings. Each of the four control group wound sites were covered with small squares ($\sim 10\,mm^2$) of sterile, petrolatum jelly–impregnated gauze[7] and further secured with Tegaderm® (3M Corporation, St. Paul, MN)[9,18] to serve as an impermeable moisture barrier and wound cover.[2] Each of the six treatment group wound sites received an ADSC-seeded electrospun tropoelastin membrane that was then covered by a small square of petrolatum gauze and secured with Tegaderm, in like manner to control group wound sites.

Perioperative care of experimental animals

All mice were housed in individually ventilated caging with high-efficiency particulate arresting filtration at cage level. Cages were thoroughly sanitized, and bedding materials were autoclaved before use. Mice were housed individually. Food was sterilized via irradiation, and drinking water was supplemented with sulfamethoxazole/trimethoprim calculated to provide a dosage of 95 mg/kg per day. Welfare checks were performed at least twice daily, and postoperative analgesics were administered as needed.

Standard histology

At postoperative day 6, specimens of each wound site were removed immediately post mortem with 10-mm biopsy punches and placed into 2% paraformaldehyde for 24-h fixation. Specimens were subsequently dried and paraffin embedded. Sectioning of specimens was performed at a thickness of 7 μm, followed by hematoxylin-eosin staining.

Immunohistochemical staining

Paraffin-embedded blocks of each specimen were reacted with a polyclonal antibody for anti–von Willebrand factor for identification of microvessels (anti–von Willebrand antibody ab6994, Abcam, Cambridge, MA). Slides were then digitally scanned for microscopic assessments using an Aperio Scanscope CS scanner (Leica Biosystems, Vista, CA).

Image capture and analysis

Culture sample images were captured using an Olympus model CK2 inverted phase-contrast light microscope (Olympus America Inc., Melville, NY). Initial imaging of naked electrospun tropoelastin membranes was performed at the Northern Arizona University Imaging and Histology Core Facility, using a Leo 435 VP scanning electron microscope (Leo Electron Microscopy Inc., Thornwood, NY). Imaging of ADSC-seeded electrospun membranes was performed at the LeRoy Eyring Center for Solid State Science at Arizona State University, using an FEI model XL-30 scanning electron microscope (FEI Company, Hillsboro, OR). Images of each wound site were obtained at postoperative days 0 and 6 during the *in vivo* portion of this study. A metric ruler was placed next to each wound site and photographed with a high-resolution digital camera (EOS model, Canon USA, Inc., Melville, NY)[19] outfitted with a Sigma DG Macro Lens (Sigma Corp. of America, Ronkonkoma, NY) and a Neewer ring light (Neewer, Edison, NJ).

Digital images of postoperative day 0 and 6 wounds were analyzed using ImageJ software (ImageJ, National Institutes of Health, Bethesda, MD).[7,18] The edges of each wound, defined by the perimeter of grossly apparent re-epithelialization, were traced manually.[19] Wound area was calculated using the area analysis software. The software was recalibrated for each digital image using the metric ruler in the image backdrop as a reference scale. The following was used to calculate percent wound closure:[18]

$$\frac{\text{Initial Wound Area} - \text{Final Wound Area}}{\text{Initial Wound Area}} \times 100\%$$

Digital histology images were analyzed for re-epithelialization with Aperio ImageScope software (Leica Biosystems, Vista, CA).

Statistical analysis

Analyses were performed using JMP Pro-10 statistical computation software (SAS Institute Inc., Cary, NC). Statistically significant differences were determined by a Student's *t*-test. Statistical significance was determined by $p \le 0.05$. Data are presented as means ± standard error.

RESULTS

Images of naked scaffolds

Scanning electron micrographs of the electrospun tropoelastin membranes revealed the characteristic open weave pattern of protein fibers with diameters in the submicron range (Fig. 1). In agreement with prior studies,[20,21] we observed changes in final scaffold porosity when using different protein solution ejection rates during electrospinning.

Gross observations and microscopic images of ADSC-seeded scaffolds

There was no appreciable disintegration of the non-crosslinked tropoelastin membranes observed over the 6-day incubation phase in aqueous cell culture media. Scanning electron micrographs of ADSC-seeded electrospun tropoelastin (crosslinked and non-crosslinked) revealed exceptional biocompatibility of these materials. This is demonstrated

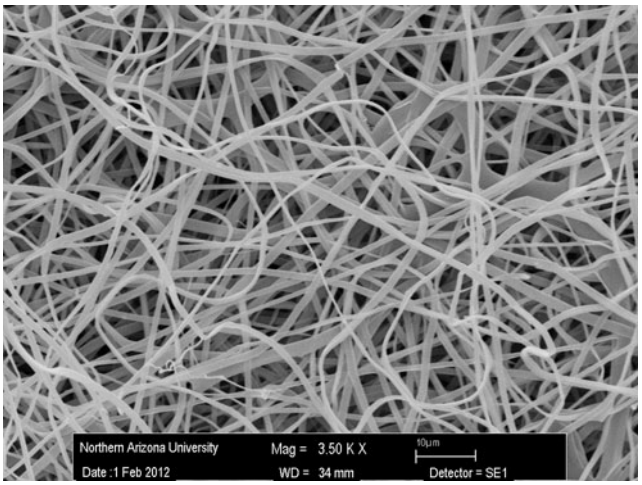

Figure 1. Representative scanning electron micrograph that illustrates the microarchitecture of electrospun tropoelastin (rhTE) scaffold. Scale bar = 10 μm.

by the flattened morphology of the ADSCs,[4] obvious conformation to substrate topography, and their notable deposition of a new ECM (Fig. 2).[22–25] These results demonstrate that electrospun rhTE (noncrosslinked) and glutaraldehyde (crosslinked) are noncytotoxic and may be suitable cell carriers for therapeutic ADSC administration.

In vivo wound healing

Gross measurements. The physiological response of ADSC-seeded electrospun tropoelastin membranes were studied in a murine excisional wound model and compared to treatment with sterile petrolatum gauze and Tegaderm as a control. Digital photographs of the wound sites were taken directly after wound creation (day 0) and immediately after euthanization on postoperative day 6. The surface area of each wound was analyzed using ImageJ software (Fig. 3A). Wounds treated with rhTE plus ADSC displayed significantly greater wound closure than controls ($p < 0.02$; Fig. 3B, C). The average percent wound closure for control and rhTE + ADSC groups were $74.5 \pm 13.7\%$ and $93.8 \pm 9.4\%$, respectively (Fig. 3D).

Histologic measurements. Specimens of each wound site were sectioned, mounted, and stained. Digital histology images of each wound site were analyzed for epithelial thickness. Mean thickness of re-epithelialized tissue for control and rhTE + ADSC–treated wound sites were 27.7 ± 7.8 μm and 51.9 ± 11.27 μm, respectively (Fig. 4). Thus, wounds treated with rhTE + ADSC displayed significantly greater epithelial thickness than controls ($p = 0.001$; Figs. 4 and 5). This is evident from the immunohistochemistry where minimal new epithelium can be seen in control wound sites compared to rhTE + ADSC–treated wound sites (Fig. 5, brackets). In rhTE + ADSC–treated wound sites, within the newly present epithelium, hallmark stratum layers of the mouse epidermis are present. Specifically, a new stratum corneum layer is present (Fig. 5, green arrows).

DISCUSSION

Current clinical treatments for full-thickness dermal trauma, such as lacerations, avulsions, third- and fourth-degree burns, and tumor excisions, are far from ideal. Healed tissue is typically marred by extensive scarring and contraction, inhibiting normal movement and rendering the healed integument aesthetically unappealing. Open wounds may persist for years in diabetic patients as nonhealing ulcers. Although elastin and elastin-derived peptides have demonstrated promising mechanical and biochemical attributes for use as wound dressings, currently available dermal substitutes lack this vital integumentary protein.[3]

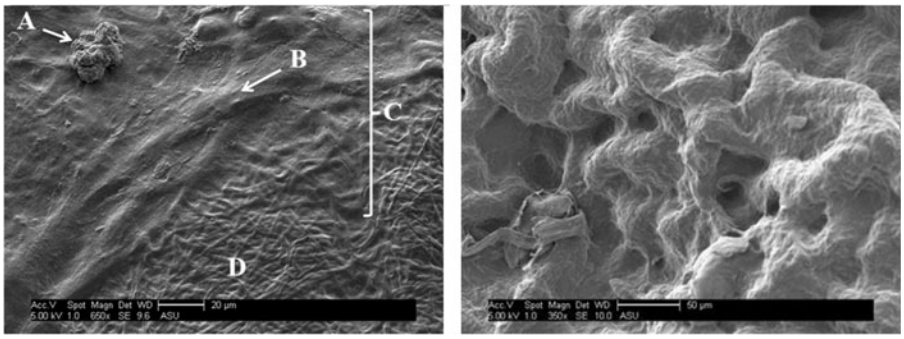

Figure 2. *Left*: Representative image of electrospun rhTE (glutaraldehyde crosslinked) + hADSC, in which the dividing hADSC (A), an hADSC "bump" (i.e., flattened cell body) within ECM (B), a new ECM deposition (C), and the bare rhTE scaffold (D) are shown (scale bar = 20 μm). *Right:* Higher magnification view of electrospun rhTE with newly created ECM from seeded hADSCs. Scale bar = 50 μm.

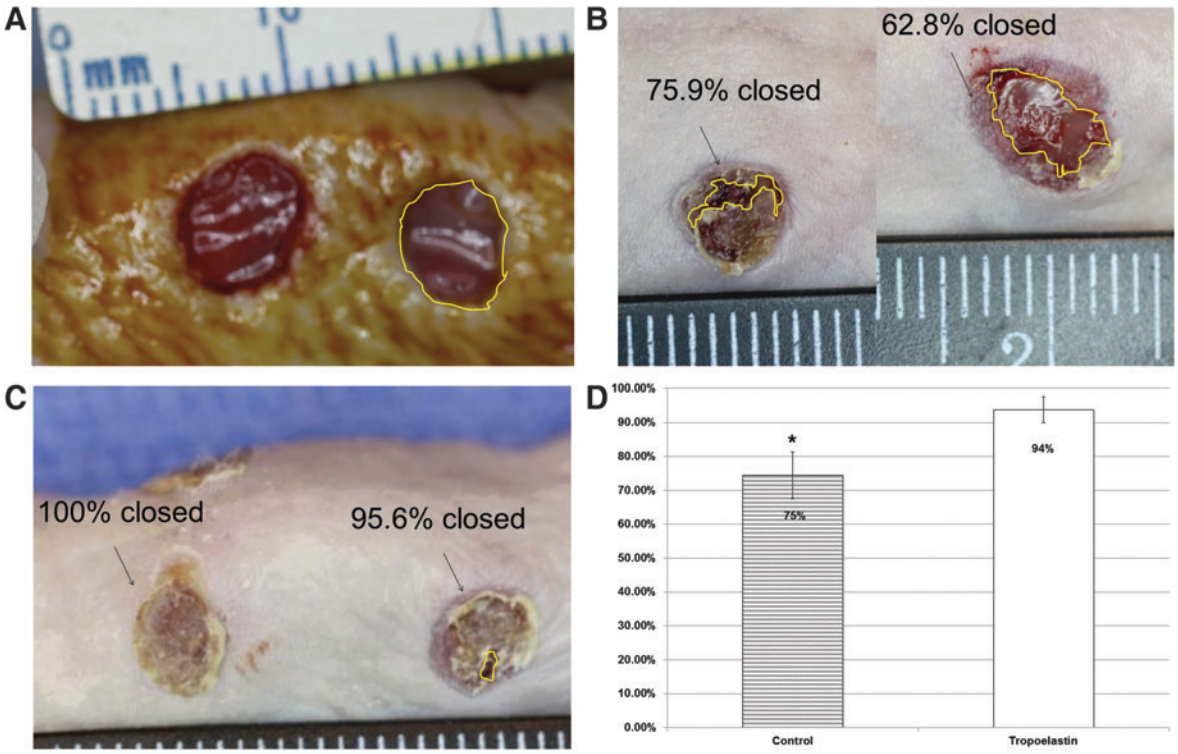

Figure 3. **(A)** Example of circumscribed wound area using ImageJ software. Pretreatment wound area. **(B)** Representative image at the day 6 time point in the control group. **(C)** Representative image of the rhTE plus hADSC treatment group. **(D)** Average percent wound closure in the control versus rhTE + hADSC treatment groups ($p < 0.02$). To see this illustration in color, the reader is referred to the web version of this article at www.liebertpub.com/wound

Human adipose-derived stem cells (hADSCs) have shown considerable promise in the treatment of dermal wounds, but no optimal delivery device has yet to be identified. Considering that a stem cell's differentiation and cytokine expression is largely mediated by the mechanical and biochemical properties of its immediate environment, we hypothesize that an elastin-based scaffold may be a superior delivery vehicle for therapeutic hADSCs. It is noteworthy that wound sites treated with ADSC-seeded electrospun rhTE scaffolds displayed significantly faster wound closure than controls. These results were confirmed by histologic analysis, and the thickness of new epithelium in ADSC-treated wounds was significantly greater than those of control group wounds.

Microvessel density analysis demonstrated significantly higher values in the control group compared to the treatment group (data not shown). As the role of angiogenesis in wound healing is temporary and angioregression represents a later stage of wound repair,[26] it is possible that the lower microvessel densities observed in the treatment group correspond to more rapid progression through the phases of normal wound healing. This would need to be explored with future studies and additional time points, however.

It is becoming increasingly apparent that the mechanical characteristics of a biomaterial are critical factors to consider for tissue engineering and wound-healing applications. The majority of currently available dermal substitutes are collagen-based scaffolds, which are hampered by a deficit in elasticity as well as pronounced scaffold contraction and scar formation *in vivo*.[3,20] Recent experiments in a collaborating laboratory highlight the unique mechanical properties of rhTE; electrospun rhTE scaffolds display much lower stiffness and higher elastic moduli than electrospun collagen scaffolds.[27] Considering the elastic nature of the integument (as well as many other tissues and organs), the use of rhTE in a wound dressing may be superior to collagen-based scaffolds for long-term use, especially when the said scaffold is intended to integrate with the host tissue for long-term tissue regeneration. A tropoelastin-based scaffold also may persist in the scar tissue and enhance the strength and elasticity of the healed scar. Additional research on the quality of a scar formed in the presence of this substrate is warranted.

The properties of a delivery substrate affect stem cell lineage differentiation. Previous research has shown that type 1 collagen–based materials induce osteogenic[28,29] and chondrogenic[30] differentiation

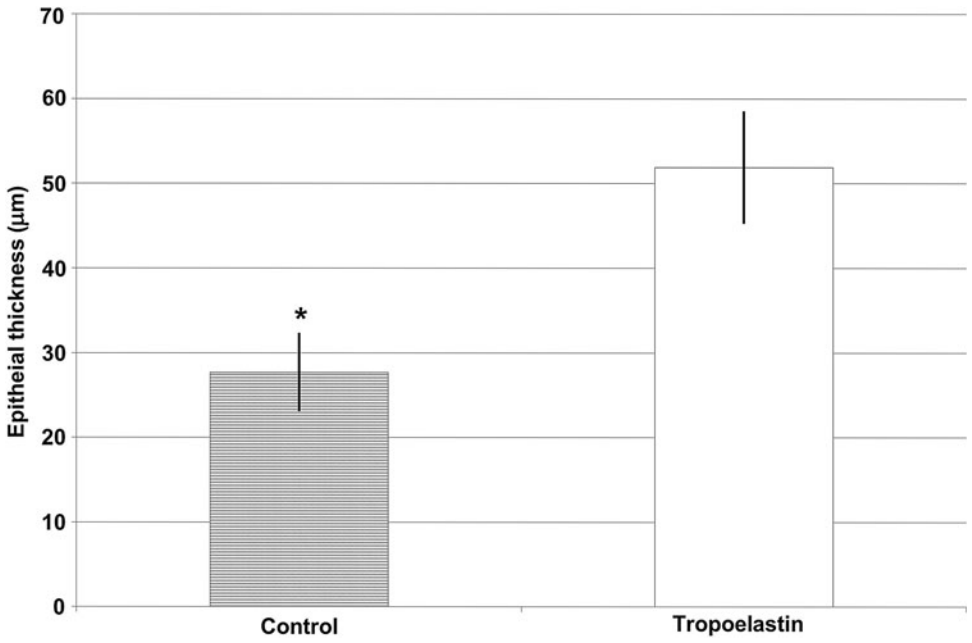

Figure 4. Average epithelial thickness (μm) measurements in the control versus rhTE+hADSC treatment groups ($p=0.001$).

of various stem cell types. This is an undesirable effect for the healing or regeneration of non-osteogenic or non-chondrogenic tissues. This does not imply that rhTE would be superior to collagen for lineage induction of therapeutic stem cells. More research is required to determine the effects of rhTE upon lineage differentiation of ADSCs, as well as other stem cell lines.

The use of collagen in a therapeutic stem cell delivery vehicle may also be contraindicated for use in other organ systems, where excessive collagen deposition or collagen-mediated thrombogenicity contributes to a pathologic state. For example, in a postinfarcted heart, necrotic myocardium is replaced with collagen-based scar tissue, decreasing elasticity, and inhibiting diastolic function.[31] Thus, the administration of additional collagen proteins via a stem cell delivery vehicle may be counterproductive. To this point, in two recent studies using a rat myocardial infarct model, hearts treated with stem cells genetically modified to overexpress tropoelastin significantly attenuated scar development, preserved the integrity of the ECM, reduced ventricular dilation, and increased ejection fraction compared to controls.[31,32]

It is not unreasonable to propose that the benefits of tropoelastin in tissue engineering and regeneration have only begun to be discovered. In the ongoing quest to synthesize dermal substitutes *in vitro*, inclusion of this pivotal protein is certainly

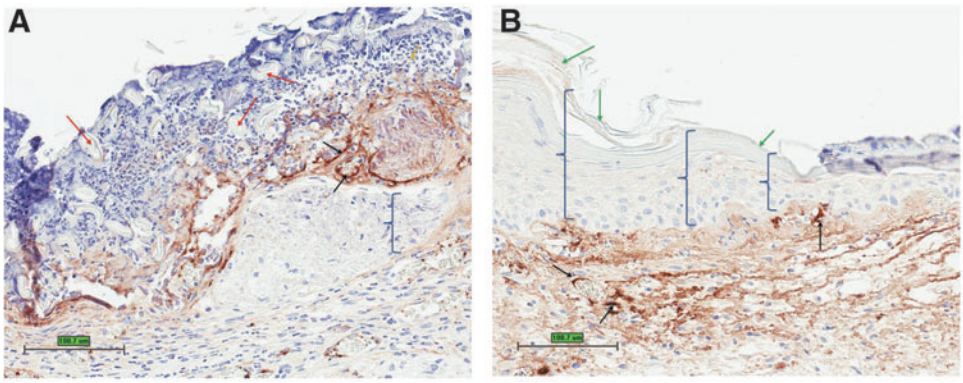

Figure 5. **(A)** Representative control treatment group immunohistochemistry reacted with Von Willebrand factor. **(B)** Representative rhTE+hADSC treatment group immunohistochemistry reacted with Von Willebrand factor. Red arrows=Vaseline gauze; black arrows=new microvasculature; green arrows=new stratum corneum; brackets=new epithelium. Scale bars=100 μm. To see this illustration in color, the reader is referred to the web version of this article at www.liebertpub.com/wound

warranted. Additionally, further elucidation of tropoelastin's chemokine/matrikine properties, particularly in relation to lineage induction of therapeutic stem cell lines, is expected to reveal further intriguing findings. Of paramount importance, however, we truly hope that further research on tropoelastin, therapeutic stem cells, and ECM mimetics will ultimately lead to improved clinical therapies for victims of burns, severe dermal trauma, and other daunting pathologies.

KEY FINDINGS

- Electrospun tropoelastin membranes form stable structures that retain their integrity and strength in tissue culture medium.
- These membranes can be populated *in vitro* by hADSCs.
- The cells rapidly proliferate on the scaffold and secrete an ECM that eventually covers the entire scaffold, including the cells.
- The populated scaffold is well tolerated in a murine excisional wound model.
- Wounds treated with the ADSC-populated tropoelastin scaffolds displayed a significantly greater rate of closure and restoration of normal epithelium.

LIMITATIONS OF THE CURRENT STUDY

In the current study, hADSCs alone, rhTE alone, and splinted wounds were not performed. Delivering hADSCs alone to wounds presents cellular retention challenges in the wound. Therefore, this treatment group was not enrolled in the current study. As a result, the specific role hADSCs play in the current study results cannot be determined. Likewise, without a separate rhTE treatment group, we are unable to attribute the role the scaffold alone is contributing in the current study; the reported results are instead due to a combination of rhTE scaffold and hADSCs. Careful interpretation is required surrounding the overall wound-healing results; we cannot separate out wound contraction and wound-healing contributions to the overall results. Because a splinting model was not used in the current study design, wound contraction due to the underlying subcutaneous panniculus carnosus layer in the mouse is most likely present along with wound healing events.

INNOVATION

This is the first report on the use of tropoelastin-based biomaterials as delivery vehicles for therapeutic ADSCs to treat full-thickness wounds. The mechanical and biochemical characteristics of tropoelastin can offer unique, beneficial properties to a healing wound bed. Current clinical therapies for the treatment of dermal wounds are limited in their ability, and not all wounds are successfully treated without scarring and/or appropriate aesthetic results. Therefore, there is a well established clinical need for continued improvement and innovation in this field.

ACKNOWLEDGMENTS AND FUNDING SOURCES

We would like thank Protein Genomics for supplying recombinant tropoelastin for this research along with reagents and use of their laboratory space. We would like to thank American CryoStem Corporation for supplying cryopreserved ADSCs for these studies. We acknowledge the National Science Foundation Major Research Instrumentation Grant #1126742, which allowed for SEM imaging access at Northern Arizona University.

AUTHOR DISCLOSURE AND GHOSTWRITING

No competing financial interests exist for H.M. B.E. and R.K. have financial interests in Protein Genomics. The content of this article was expressly written by the authors listed. No ghostwriters were used to write this article.

ABOUT THE AUTHORS

Hans Machula was a graduate student at the time this research was completed. The data within this manuscript were a part of Mr. Machula's graduate research at Northern Arizona University. Mr. Machula is currently in medical school at Rocky Vista University College of Osteopathic Medicine in Parker, Colorado. **Burt D. Ensley, PhD,** is the CEO and Chairman of Protein Genomics, a privately held biomaterials company. He has held this position since 2004. Dr. Ensley has held various positions in the private sector since completing his postdoctoral work in 1981. **Robert S. Kellar, PhD,** is the founder and President of Development Engineering Sciences, a bioengineering consulting firm. He holds a full-time faculty position at Northern Arizona University in the Department of Biological Sciences and an adjunct faculty appointment in Mechanical Engineering. He has held various positions at biotechnology and medical devices companies and currently serves on numerous boards and scientific advisory boards.

REFERENCES

1. Ruszczak Z and Schwartz RA: Modern aspects of wound healing: an update. Dermatol Surg 2000; **26:** 219.
2. van der Veen VC, van der Wal MB, van Leeuwen MC, Ulrich MM, and Middelkoop E: Biological background of dermal substitutes. Burns 2010; **36:** 305.
3. Rnjak J, Wise SG, Mithieux SM, and Weiss AS: Severe burn injuries and the role of elastin in the design of dermal substitutes. Tissue Eng Part B Rev 2011; **17:** 81.
4. Mizuno H: Adipose-derived stem cells for tissue repair and regeneration: ten years of research and a literature review. J Nippon Med Sch 2009; **76:** 56.
5. Beeson W, Woods E, and Agha R: Tissue engineering, regenerative medicine, and rejuvenation in 2010: the role of adipose-derived stem cells. Facial Plast Surg 2011; **27:** 378.
6. Nie C, Yang D, Xu J, Si Z, Jin X, and Zhang J: Locally administered adipose-derived stem cells accelerate wound healing through differentiation and vasculogenesis. Cell Transplant 2011; **20:** 205.
7. Liu S, Zhang H, Zhang X, *et al.*: Synergistic angiogenesis promoting effects of extracellular matrix scaffolds and adipose-derived stem cells during wound repair. Tissue Eng Part A 2011; **17:** 725.
8. Ebrahimian TG, Pouzoulet F, Squiban C, *et al.*: Cell therapy based on adipose tissue-derived stromal cells promotes physiological and pathological wound healing. Arterioscler Thromb Vasc Biol 2009; **29:** 503.
9. Kim WS, Park BS, Sung JH, *et al.*: Wound healing effect of adipose-derived stem cells: a critical role of secretory factors on human dermal fibroblasts. J Dermatol Sci 2007; **48:** 15.
10. Naughton GK and Kellar RS: Human ECM for medical devices and therapeutics. Medical Device and Diagnostic Industry. May 2008. www.mddionline.com/article/human-ecm-devices-and-therapeutics.
11. Brayfield C, Marra K, and Rubin JP: Adipose stem cells for soft tissue regeneration. Handchir Mikrochir Plast Chir 2010; **42:** 124.
12. Senior RM, Griffin GL, and Mecham RP: Chemotactic activity of elastin-derived peptides. J Clin Invest 1980; **66:** 859.
13. Almine JF, Wise SG, and Weiss AS: Elastin signaling in wound repair. Birth Defects Res Part C Embryo Today Rev 2012; **96:** 248.
14. Fujimoto N, Tajima S, and Ishibashi A: Elastin peptides induce migration and terminal differentiation of cultured keratinocytes via 67 kDa elastin receptor in vitro: 67 kDa elastin receptor is expressed in the keratinocytes eliminating elastic materials in elastosis perforans serpiginosa. J Investig Dermatol 2000; **115:** 633.
15. Mochizuki S, Brassart B, and Hinek A: Signaling pathways transduced through the elastin receptor facilitate proliferation of arterial smooth muscle cells. J Biol Chem 2002; **277:** 44854.
16. Hinek A, Wang Y, Liu K, Mitts TF, and Jimenez F: Proteolytic digest derived from bovine Ligamentum Nuchae stimulates deposition of new elastin-enriched matrix in cultures and transplants of human dermal fibroblasts. J Dermatol Sci 2005; **39:** 155.
17. Matthews JA, Wnek GE, Simpson DG, and Bowlin GL: Electrospinning of collagen nanofibers. Biomacromolecules 2002; **3:** 232.
18. Dubský M, Kubinová S, Sirc J, *et al.*: Nanofibers prepared by needleless electrospinning technology as scaffolds for wound healing. J Mater Sci Mater Med 2012; **23:** 931.
19. Altman AM, Yan Y, Matthias N, *et al.*: IFATS collection: human adipose-derived stem cells seeded on a silk fibroin-chitosan scaffold enhance wound repair in a murine soft tissue injury model. Stem Cells 2009; **27:** 250.
20. Rnjak-Kovacina J, Wise SG, Li Z, *et al.*: Tailoring the porosity and pore size of electrospun synthetic human elastin scaffolds for dermal tissue engineering. Biomaterials 2011; **32:** 6729.
21. Rnjak J, Li Z, Maitz PK, Wise SG, and Weiss AS: Primary human dermal fibroblast interactions with open weave three-dimensional scaffolds prepared from synthetic human elastin. Biomaterials 2009; **30:** 6469.
22. Liu Q, Cen L, Yin S, *et al.*: A comparative study of proliferation and osteogenic differentiation of adipose-derived stem cells on akermanite and beta-TCP ceramics. Biomaterials 2008; **29:** 4792.
23. McCullen SD, Stevens DR, Roberts WA, *et al.*: Characterization of electrospun nanocomposite scaffolds and biocompatibility with adipose-derived human mesenchymal stem cells. Int J Nanomedicine 2007; **2:** 253.
24. Zhu Y, Liu T, Song K, Jiang B, Ma X, and Cui Z: Collagen-chitosan polymer as a scaffold for the proliferation of human adipose tissue-derived stem cells. J Mater Sci Mater Med 2009; **20:** 799.
25. Girandon L, Kregar-Velikonja N, Božikov K, and Barlic A: In vitro models for adipose tissue engineering with adipose-derived stem cells using different scaffolds of natural origin. Folia Biol (Praha) 2011; **57:** 47.
26. Gurtner GC, Werner S, Barrandon Y, and Longaker MT: Wound repair and regeneration. Nature 2008; **453:** 314.
27. Ford A, Machula H, Kellar R, and Nelson BA: Characterizing the mechanical properties of tropoelastin protein scaffolds [abstract]. Proceedings of the Material Research Society 2013 Spring Conference, San Francisco, CA.
28. Krawetz RJ, Taiani JT, Wu YE, *et al.:* Collagen I scaffolds cross-linked with beta-glycerol phosphate induce osteogenic differentiation of embryonic stem cells in vitro and regulate their tumorigenic potential in vivo. Tissue Eng Part A 2012; **18:** 1014.
29. Lund AW, Stegemann JP, and Plopper GE: Mesenchymal stem cells sense three dimensional type I collagen through discoidin domain receptor 1. Open Stem Cell J 2009; **1:** 40.
30. Zhang L, Yuan T, Guo L, and Zhang X: An in vitro study of collagen hydrogel to induce the chondrogenic differentiation of mesenchymal stem cells. J Biomed Mater Res Part A. 2012; **100:** 2717.
31. Uchinaka A, Kawaguchi N, Hamada Y, *et al.*: Transplantation of elastin-secreting myoblast sheets improves cardiac function in infarcted rat heart. Mol Cell Biochem 2012; **368:** 203.
32. Li SH, Sun Z, Guo L, *et al.*: Elastin overexpression by cell-based gene therapy preserves matrix and prevents cardiac dilation. J Cell Mol Med 2012; **16:** 2429.

Abbreviations and Acronyms

ADSC = adipose-derived stem cell
ECM = extracellular matrix
hADSC = human adipose-derived stem cell
HFIP = hexafluoroisopropanol
rhTE = recombinant human tropoelastin
SEM = scanning electron microscopy